

High-Speed Limit Cycle Walking for Biped Robots using Active Up-and-Down Motion Control of Wobbling Mass

Yuta Hanazawa¹, Terumitsu Hayashi¹, Masaki Yamakita¹ and Fumihiko Asano²

Abstract—In this paper, we propose a novel method for fast limit cycle walking using active control of a wobbling mass. Limit cycle walkers achieving energy-efficient walking have been developed in the last decade. Many researchers have recently studied methods for improving walking speed of limit cycle walkers. In human walking, humans swing their arms according to walking phases and the motion is a regularly symmetric motion about the torso. We consider that this motion is an active up-and-down motion for a mass and improves biped walking speed. We numerically and mathematically show that a biped robot achieves fast limit cycle walking by the proposed method.

I. INTRODUCTION

Biped robots can easily change walking directions even in narrow spaces and walk on various environments. These properties are excellent as mobile robots and we thus want to develop a biped robot that achieves fast, energy-efficient and robust dynamic walking anywhere.

Many researchers have studied biped robots that achieve robust dynamic walking in uneven terrains and stairs [1], [2], [3]. Biped robots achieving energy-efficient walking also have been studied in the last decade. One of the approaches is active walking based on energy-efficient passive dynamic walking [4] and this walking is called limit cycle walking [5], [6], [7], [8], [9], [10].

Limit cycle walkers achieve more energy-efficient biped walking than many recent biped robots using their own dynamics and small amount of energy [11]. Methods for improving walking speed of limit cycle walkers have also been studied since their walking speed are, generally, slower than those of many recent biped robots (e.g., ASIMO [1], PETMAN [3]).

Asano et al. have shown fast limit cycle walking using effects of arc-feet [12], and they have also shown fast limit cycle walking using parametric excitation mechanism [13]. Hobbelen et al. have developed a limit cycle walker with ankle springs [14], [15], [16], and this limit cycle walker has achieved high-speed walking using posture of the upper-body [15]. Hanazawa et al. have shown that a biped robot has more appropriate ankle impedance for high-speed walking by the ankle springs and inerters [17], [18], and they also developed

¹Y. Hanazawa, ¹T. Hayashi, ¹M. Yamakita are with the Dept. of Mechanical and Control Engineering, Tokyo Institute of Technology, 2-12-1 Oh-okayama, Meguro-ku Tokyo 152-8552, JAPAN, and Y. Hanazawa is now working for Kyushu Institute of Technology hanazawa-y@ise.kyutech.ac.jp, {hayashi, yamakita}@ac.ctrl.titech.ac.jp

²F. Asano is with the School of Information Science, Japan Advanced Institute of Science and Technology, 1-1 Asahidai, Nomi, Ishikawa 923-1292, JAPAN fasano@jaist.ac.jp

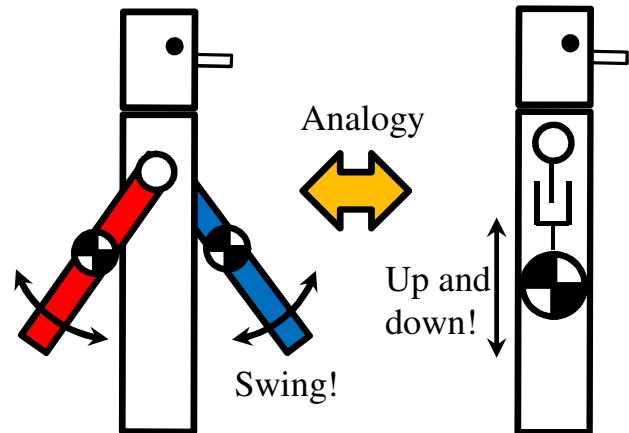


Fig. 1. Analogy of swinging arms and wobbling mass

a limit cycle walker with ankle springs and inerters [19]. This walker has achieved fast limit cycle walking by appropriate ankle impedance for high-speed walking due to the ankle springs and inerters.

Although these approaches are effective for increasing walking speed, we want to achieve a more high-speed limit cycle walker by the conventional methods in combination with novel other methods. To achieve a more high-speed limit cycle walker than conventional limit cycle walkers, we must thus develop a novel method that is very different from the conventional methods for improving walking speed.

We consider that up-and-down motions of a wobbling mass during walking improve walking speed as the method. Rome et al. have shown that walking performance of humans with a heavy backpack is improved by up-and-down motions of the backpack using elastic elements [20]. Tanaka et al. have shown increasing walking speed of a combined rimless wheel that can be achieved by using up-and-down motions of a wobbling mass [21]. We also notice that swinging arms in human walking are similar to the up-and-down motions of a wobbling mass when we observe human walking from sagittal plane (i.e., 2D-plane) as shown in Fig. 1. This active motions are not an irregular pattern but a regular pattern according to walking phase. Moreover, humans change the amplitude of the swinging arms according to walking speed, and this amplitude is small in slow walking and big in fast walking.

We thus strongly infer that the regular active up-and-down motions of a wobbling mass like swinging arms improve walking speed. In this paper, we propose a novel method for

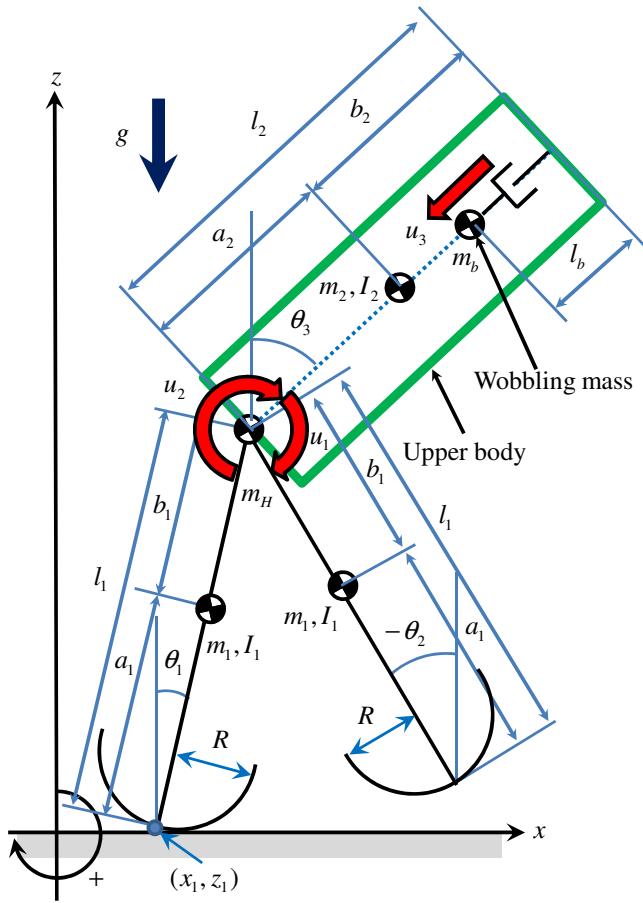


Fig. 2. Model of biped robot with upper-body and wobbling mass

improving walking speed using active control of a wobbling mass. We show the validity of the proposed method through numerical simulations and mathematical analyses.

II. MODEL OF BIPED ROBOT

A. Dynamic equation

Fig. 2 shows the model of a biped robot with arc-feet and an upper-body that consists of a torso frame and wobbling mass. The wobbling mass can move up and down with respect to the torso by the actuator. This robot also has two actuators for active control of the upper-body and swing-leg. Dynamic equation of the robot is given by

$$M(\mathbf{q})\ddot{\mathbf{q}} + C(\mathbf{q}, \dot{\mathbf{q}})\dot{\mathbf{q}} + \mathbf{G}(\mathbf{q}) = \mathbf{S}_1 \mathbf{u} + \mathbf{J}_c(\mathbf{q})^T \boldsymbol{\lambda}, \quad (1)$$

where $\mathbf{q} = [\theta_1, \theta_2, \theta_3, l_b, x_1, z_1]^T$ is the generalized coordinate vector, $M(\mathbf{q}) \in \mathbb{R}^{6 \times 6}$ is an inertia matrix, $C(\mathbf{q}, \dot{\mathbf{q}}) \in \mathbb{R}^{6 \times 6}$ is a Coriolis and centrifugal force matrix, $\mathbf{G}(\mathbf{q}) \in \mathbb{R}^6$ is a gravitational vector, $\mathbf{u} = [u_1, u_2, u_3]^T$ is an input vector, $\mathbf{S}_1 \in \mathbb{R}^{6 \times 3}$ is the driving matrix and is

detailed as

$$\mathbf{S}_1 = \begin{bmatrix} 0 & -1 & 0 \\ 1 & 0 & 0 \\ -1 & 1 & 0 \\ 0 & 0 & 1 \\ 0 & 0 & 0 \\ 0 & 0 & 0 \end{bmatrix}. \quad (2)$$

$\mathbf{J}_c(\mathbf{q}) \in \mathbb{R}^{N \times 6}$ is a Jacobian matrix and is determined according to the constraint conditions of the robot, N is the number of constraint conditions. $\boldsymbol{\lambda} \in \mathbb{R}^N$ is a constraint force vector given by

$$\boldsymbol{\lambda} = -\mathbf{X}(\mathbf{q})^{-1}(\mathbf{J}_c(\mathbf{q})\mathbf{M}(\mathbf{q})^{-1}\boldsymbol{\Gamma}(\mathbf{q}, \dot{\mathbf{q}}, \mathbf{u}) + \dot{\mathbf{J}}_c(\mathbf{q}, \dot{\mathbf{q}})\dot{\mathbf{q}}), \quad (3)$$

$$\mathbf{X}(\mathbf{q}) = \mathbf{J}_c(\mathbf{q})\mathbf{M}(\mathbf{q})^{-1}\mathbf{J}_c(\mathbf{q})^T, \quad (4)$$

$$\boldsymbol{\Gamma}(\mathbf{q}, \dot{\mathbf{q}}, \mathbf{u}) = \mathbf{S}_1 \mathbf{u} - \mathbf{C}(\mathbf{q}, \dot{\mathbf{q}})\dot{\mathbf{q}} - \mathbf{G}(\mathbf{q}). \quad (5)$$

B. Constraint conditions

In this paper, we analyze limit cycle walking with active control of up-and-down motions of a (unlocked) wobbling mass and a mechanically locked wobbling mass to show effectiveness of the proposed method. We also show $\mathbf{J}_c(\mathbf{q})$, $\dot{\mathbf{J}}_c(\mathbf{q}, \dot{\mathbf{q}})$ in each case.

1) *Unlocked wobbling mass case*: Since the contact point of the biped robot is constrained with ground, constraint equations are expressed as

$$R(\cos \theta_1 - 1)\dot{\theta}_1 + \dot{x}_1 = 0, \quad (6)$$

$$-R \sin \theta_1 \dot{\theta}_1 + \dot{z}_1 = 0. \quad (7)$$

From these equations, we obtain $\mathbf{J}_c(\mathbf{q}) \in \mathbb{R}^{2 \times 6}$ and $\dot{\mathbf{J}}_c(\mathbf{q}, \dot{\mathbf{q}}) \in \mathbb{R}^{2 \times 6}$ as

$$\mathbf{J}_c(\mathbf{q})\dot{\mathbf{q}} = \begin{bmatrix} R(\cos \theta_1 - 1) & 0 & 0 & 0 & 1 & 0 \\ -R \sin \theta_1 & 0 & 0 & 0 & 0 & 1 \end{bmatrix} \dot{\mathbf{q}} = \mathbf{0}_{2 \times 1}, \quad (8)$$

$$\dot{\mathbf{J}}_c(\mathbf{q}, \dot{\mathbf{q}}) = \begin{bmatrix} -R\dot{\theta}_1 \sin \theta_1 & 0 & 0 & 0 & 0 & 0 \\ -R\dot{\theta}_1 \cos \theta_1 & 0 & 0 & 0 & 0 & 0 \end{bmatrix}. \quad (9)$$

2) *Locked wobbling mass case*: When the wobbling mass is locked mechanically (i.e., $l_b = l_0$), we obtain the following constraint equation:

$$\dot{l}_b = 0. \quad (10)$$

From (6)(7)(10), $\mathbf{J}_c(\mathbf{q}) \in \mathbb{R}^{3 \times 6}$ and $\dot{\mathbf{J}}_c(\mathbf{q}, \dot{\mathbf{q}}) \in \mathbb{R}^{3 \times 6}$ are expressed as

$$\mathbf{J}_c(\mathbf{q})\dot{\mathbf{q}} = \begin{bmatrix} R(\cos \theta_1 - 1) & 0 & 0 & 0 & 1 & 0 \\ -R \sin \theta_1 & 0 & 0 & 0 & 0 & 1 \\ 0 & 0 & 0 & 1 & 0 & 0 \end{bmatrix} \dot{\mathbf{q}} = \mathbf{0}_{3 \times 1}, \quad (11)$$

$$\dot{\mathbf{J}}_c(\mathbf{q}, \dot{\mathbf{q}}) = \begin{bmatrix} -R\dot{\theta}_1 \sin \theta_1 & 0 & 0 & 0 & 0 & 0 \\ -R\dot{\theta}_1 \cos \theta_1 & 0 & 0 & 0 & 0 & 0 \\ 0 & 0 & 0 & 0 & 0 & 0 \end{bmatrix}. \quad (12)$$

C. Impact equation

We assume that the collision of the swing leg with ground is inelastic and instantaneous. We can derive the velocity immediately after the impact by solving the impact equations described in the following [22].

1) *Unlocked wobbling mass case*: Since the contact point of the biped robot is constrained with ground at the collision of the swing leg, constraint equations are expressed as

$$l_1 \cos \theta_1 \dot{\theta}_1 + ((R - l_1) \cos \theta_2 - R) \dot{\theta}_2 + \dot{x}_1 = 0, \quad (13)$$

$$-l_1 \sin \theta_1 \dot{\theta}_1 + (l_1 - R) \sin \theta_2 \dot{\theta}_2 + \dot{z}_1 = 0. \quad (14)$$

From these equations, the instantaneous constraint matrix $\mathbf{J}_I(\mathbf{q}) \in \mathbb{R}^{2 \times 6}$ at the unlocked wobbling mass case is given by

$$\mathbf{J}_I(\mathbf{q}) = \begin{bmatrix} l_1 \cos \theta_1 & (R - l_1) \cos \theta_2 - R & 0 & 0 & 1 & 0 \\ -l_1 \sin \theta_1 & (l_1 - R) \sin \theta_2 & 0 & 0 & 0 & 1 \end{bmatrix}. \quad (15)$$

2) *Locked wobbling mass case*: We obtain the following constraint equation when the wobbling mass is locked mechanically ($l_b = l_0$):

$$\dot{l}_b = 0. \quad (16)$$

From (13)(14)(16), $\mathbf{J}_I(\mathbf{q}) \in \mathbb{R}^{3 \times 6}$ at the locked wobbling mass case is given by

$$\mathbf{J}_I(\mathbf{q}) = \begin{bmatrix} l_1 \cos \theta_1 & (R - l_1) \cos \theta_2 - R & 0 & 0 & 1 & 0 \\ -l_1 \sin \theta_1 & (l_1 - R) \sin \theta_2 & 0 & 0 & 0 & 1 \\ 0 & 0 & 0 & 1 & 0 & 0 \end{bmatrix}. \quad (17)$$

Impulsive force vector, $\boldsymbol{\lambda}_I \in \mathbb{R}^N$, and a velocity vector, $\dot{\mathbf{q}}^+ \in \mathbb{R}^6$, immediately after the impact are given by

$$\boldsymbol{\lambda}_I = -\mathbf{X}_I(\mathbf{q})^{-1} \mathbf{J}_I(\mathbf{q}) \dot{\mathbf{q}}^-, \quad (18)$$

$$\mathbf{X}_I(\mathbf{q}) = \mathbf{J}_I(\mathbf{q}) \mathbf{M}(\mathbf{q})^{-1} \mathbf{J}_I(\mathbf{q})^T, \quad (19)$$

$$\dot{\mathbf{q}}^+ = (\mathbf{I} - \mathbf{M}(\mathbf{q})^{-1} \mathbf{J}_I(\mathbf{q})^T \mathbf{X}_I(\mathbf{q})^{-1} \mathbf{J}_I(\mathbf{q})) \dot{\mathbf{q}}^-, \quad (20)$$

where $\dot{\mathbf{q}}^- \in \mathbb{R}^6$ is a velocity vector immediately before the impact, N is the number of instantaneous constraint conditions at the impact. We thus use (15) for the unlocked wobbling mass case, and (17) for the locked wobbling mass case. The biped robot then changes the stance leg immediately after the impact.

Table I lists the mechanical parameters of the biped robot. We use these parameters for simulations in section 4.

III. CONTROL METHODS

A. Swing leg and upper-body posture control

We first show control methods of the swing leg and posture of the upper-body for level ground walking. We realize level ground walking of the biped robot using the following simple PD-control methods:

$$u_1 = -K_{P1}(\phi_d - (\theta_1 - \theta_2)) - K_{D1}(\dot{\theta}_2 - \dot{\theta}_1), \quad (21)$$

$$u_2 = -K_{P2}(\theta_3 - \theta_{3d}) - K_{D2}\dot{\theta}_3 + u_1, \quad (22)$$

where K_{P1} , K_{P2} , K_{D1} and K_{D2} are the control gains, ϕ_d is the desire hip-joint angle, θ_{3d} is the desire torso angle. The biped robot can raise its swing leg by (21) and maintain the desired torso angle by (22).

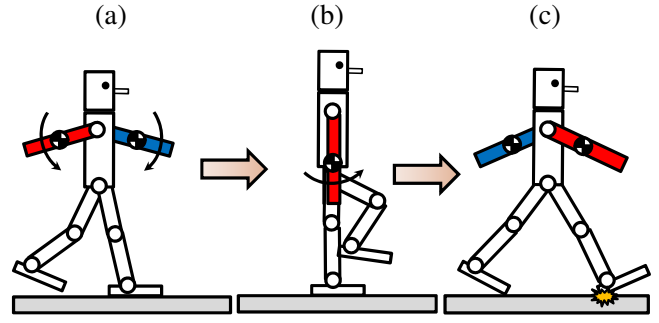


Fig. 3. Biped walking with active swinging arms

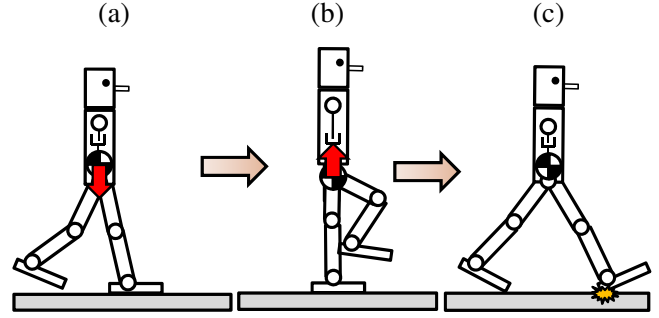


Fig. 4. Biped walking with active wobbling mass

B. Up-and-down motion control for wobbling mass

For achieving up-and-down motions of the wobbling mass, we consider swinging arms in human walking. Fig. 3 shows a schematic illustration of human walking with swinging arms. Mass points of both arms go down from the initial position immediately after the heel-strike collision as shown in Fig. 3(a), and they come at the lowest point on the mass point trajectories with respect to the torso when the stance leg is vertical as shown in Fig. 3(b). The mass points then go up by the next heel-strike collision as shown in Fig. 3(c). These relationships do not depend on walking speed and humans regularly swing their arms according to walking phase. Moreover, the amplitude of the up-and-down motion

TABLE I
MECHANICAL PARAMETERS

Symbol	Unit	Value
l_0	m	0.25
l_1	m	1.0
l_2	m	1.0
$a_1 = b_1 = l_1/2$	m	0.5
$a_2 = b_2 = l_2/2$	m	0.5
R	m	0.1
m_1	kg	5.0
m_2	kg	5.0
m_H	kg	5.0
m_b	kg	2.5
I_1	kg·m ²	4.17×10^{-1}
I_2	kg·m ²	4.17×10^{-1}

of the mass points is big when the walking is fast, and it is small when the walking is slow.

We thus consider the serial motion as an active up-and-down motion control of a wobbling mass as shown in Fig. 4. The wobbling mass goes down from the initial position immediately after the heel-strike collision as shown in Fig. 4(a), and it comes at the lowest point on the trajectory of wobbling mass with respect to the torso when the stance leg is vertical as shown in Fig. 4(b). Moreover, the wobbling mass goes up by the next heel-strike collision as shown in Fig. 4(c). Since we see that this motion is antiphase with respect to the up-and-down motion of the mass point of the torso, we propose a control method that generates this antiphase up-and-down motion of a wobbling mass. This control input is given by

$$u_3 = -K_{P3}(l_b - l_{bd}) - K_{D3}(\dot{l}_b - \dot{l}_{bd}), \quad (23)$$

$$l_{bd} = k(p_{tz} - p_0), \quad (24)$$

where K_{P3} and K_{D3} are the control gains, l_{bd} is the desire trajectory function for the wobbling mass, p_{tz} is the position (height) of the mass point of the torso (m_2), p_0 is the position offset, k is the gain.

Table II shows the control parameters in the numerical simulations. We decided the values empirically.

IV. WALKING ANALYSIS

A. Increasing walking speed by proposed method

In this section, we show effectiveness of the proposed method by a numerical simulation. Fig. 5(a) shows the angle of the stance leg, Fig. 5(b) shows the height of the mass point of the torso (i.g., m_2 in Fig. 2) and Fig. 5(c) shows the height (amplitude) of the up-and-down motion of the wobbling mass with respect to walking time. We can see that the phase of the up-and-down motion of the wobbling mass is almost antiphase with respect to that of the mass point of the torso by the proposed control method.

Table III lists the walking speed without a wobbling mass, that with a mechanically locked wobbling mass, and that with an actively controlled wobbling mass according to the proposed method. We see that the walking speed without a mass is faster than that with a mechanically locked wobbling mass. We can also see that the walking speed with an active control wobbling mass is much faster than that without a wobbling mass.

This result clearly shows the effectiveness of our proposed method and we see that the active antiphase up-and-down

TABLE II
CONTROL PARAMETERS

Symbol	Value	Symbol	Value
K_{P1}	100	θ_{3d}	0.00 [rad]
K_{D1}	25	K_{P3}	100
K_{P2}	300	K_{D3}	25
K_{D2}	50	k	6
ϕ_d	0.60 [rad]	p_0	8.7/6 [m]

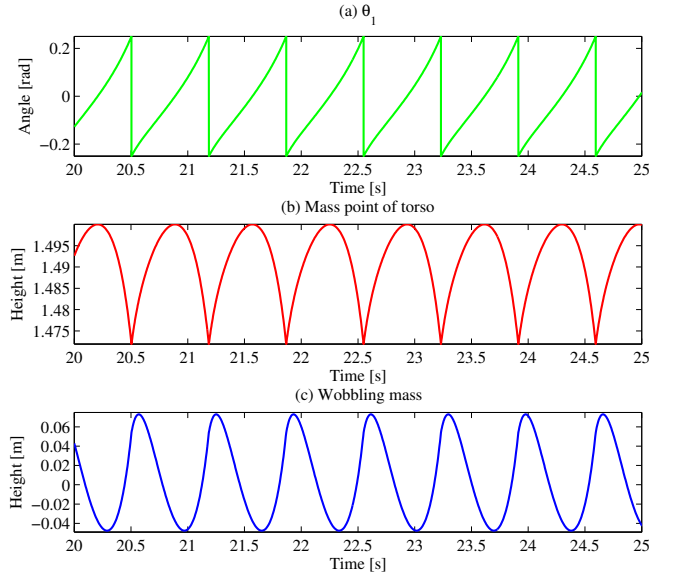


Fig. 5. Angle of stance leg, height of mass point of torso and up-and-down motion of wobbling mass with respect to time

TABLE III
SIMULATION RESULTS

Walking type	Walking speed [m/s]
without wobbling mass	0.59
with locked wobbling mass	0.51
with active wobbling mass (proposed)	0.73

motion of a wobbling mass increases speed of limit cycle walking. In the next subsection, we discuss the speeding-up mechanism mathematically.

B. Mechanism of increasing walking speed

We consider reaction force due to up-and-down motions of the wobbling mass to show a speeding-up mechanism by our proposed method. We first define a position vector from the origin to the mass point of torso (m_2) as

$$\mathbf{p}_t = \begin{bmatrix} x_1 + l_1 \sin \theta_1 + a_2 \sin \theta_3 \\ 0 \\ z_1 + l_1 \cos \theta_1 + a_2 \cos \theta_3 \end{bmatrix}, \quad (25)$$

where each x , y and z -elements of the vector are shown in Fig. 2. The y -element of the vector is 0 [m] since our model is planar. We analyze the height (i.e., z -element of the vector) of the torso during walking since the up-and-down motions of a wobbling mass are determined by the height of the mass point of the torso that is the third element of (25).

For simplicity, we assume that the arc-radius of the foot is very small ($R \approx 0$ [m]) and z_1 is nearly equal 0 [m] during walking. Moreover, our proposed method (control) almost achieves that the posture of the torso is vertical. Hence, the following relationship is satisfied since the torso angle (θ_3) is nearly equal to 0 [rad],

$$a_2 \cos(\theta_3) \approx a_2 \times 1 \approx a_2. \quad (26)$$

Therefore, the height of the mass point depends on the second term in the third element of (25), $l_1 \cos \theta_1$, and it is determined by the stance leg angle (θ_1). The height of the mass point monotonically increases with respect to time from immediately after the stance leg exchange, and it comes up a max value when the stance leg is vertical ($\theta_1 = 0$).

Then, the height of the mass point monotonically decreases with respect to time from $\theta_1 > 0$. Our proposed method achieves that the up-and-down motion of the wobbling mass is antiphase with respect to the height of the mass point of the torso, and it generates reaction force for propulsive effects of the biped walking when the angle of the stance leg is negative ($\theta_1 < 0$) as shown in Fig. 6. Moreover, it generates reaction force for propulsive effects of the biped walking when the angle of the stance leg is positive ($\theta_1 > 0$) as shown in Fig. 7.

We thus see that the reaction force due to the proposed control generates moment around the contact point of the stance leg which is given by

$$\mathbf{M} = \mathbf{r} \times \mathbf{F}, \quad (27)$$

where \mathbf{r} is a position vector from the contact point of the stance leg to the hip joint of the robot and \mathbf{F} is a vector of reaction force due to the proposed control. We can consider that the biped robot has a virtual ankle joint and this ankle generates torque for propulsive effects of the biped robot.

To more clearly show the propulsive effects, we assume that the angle of the stance leg (θ_1) is monotonically increases during the stance phase. We also assume that the reaction force of the wobbling mass is strictly positive when the angle of the stance leg is negative ($\theta_1 < 0$) and that of the wobbling mass is strictly negative when the angle of the stance leg is positive ($\theta_1 > 0$). We consider the propulsive effects in equilibrium point ($\theta_1 \approx 0$) under above assumptions, and mechanical energy due to the virtual ankle torque is given by

$$E = \int_{T_s}^{T_0} \dot{\theta}_1 (-Fl_1 \theta_1) dt + \int_{T_0}^{T_e} \dot{\theta}_1 (Fl_1 \theta_1) dt, \quad (28)$$

where T_s is a time immediately after the stance leg exchange, T_0 is a time when the angle of the stance leg is vertical and T_e is a time immediately after the collision of the swing leg (the next stance leg exchange). We see that the angle of the stance leg is negative from T_s to T_0 and positive from T_0 to T_e .

If our assumptions are satisfied, the first term of the right hand side in (28) is always positive from T_s to T_0 . Similarly, the second term of the right hand side in (28) is always positive from T_0 to T_e . We see that the virtual ankle torque generates positive mechanical energy for propulsive effects of the biped robots since these assumptions are almost satisfied by the antiphase up-and-down motion with respect to the torso mass due to our proposed control method as shown in Fig. 5. Therefore, this virtual ankle torque improves walking speed of limit cycle walking and we see that the antiphase up-and-down motion is effective for achievement of high-speed limit cycle walking.

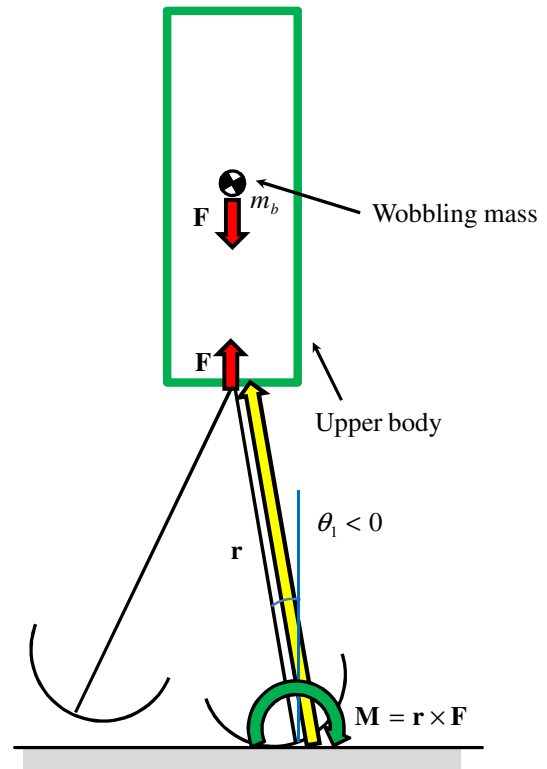


Fig. 6. $\theta_1 < 0$ (when wobbling mass is dropped)

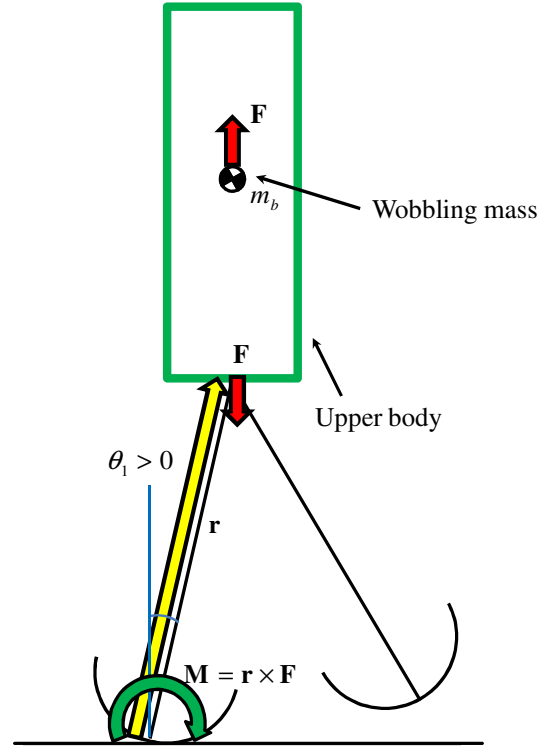


Fig. 7. $\theta_1 > 0$ (when wobbling mass is raised)

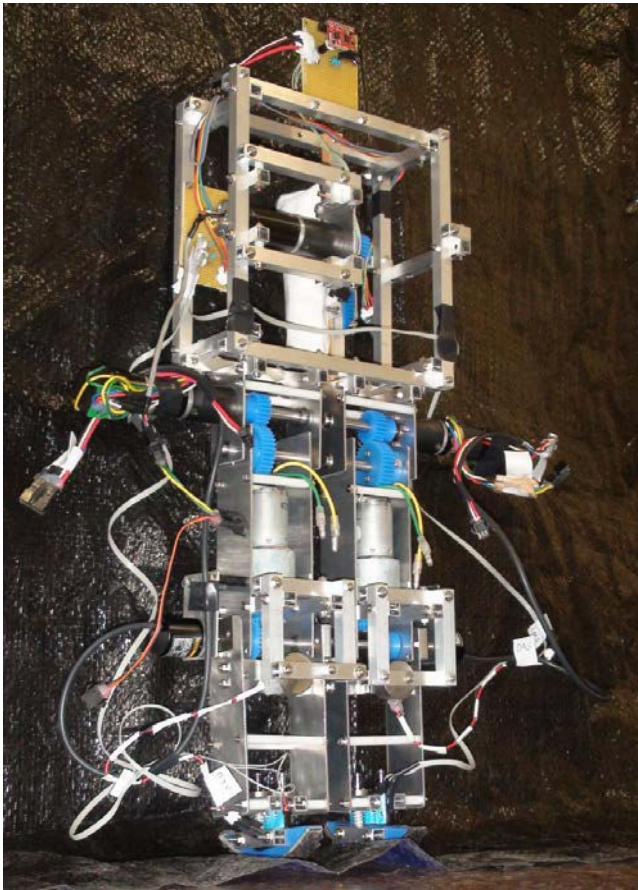


Fig. 8. Prototype of our biped robot

V. CONCLUSION AND FUTURE WORKS

In this paper, we proposed a novel method for high-speed limit cycle walking using active up-and-down motions control of a wobbling mass. We first showed that the biped robot achieves high-speed limit cycle walking by the proposed method through numerical simulations. To show the speeding-up mechanism, we mathematically analyzed the biped walking with the up-and-down motion of the wobbling mass. These results showed that the antiphase up-and-down motions of a wobbling mass with respect to that of the torso mass generates virtual torque for propulsive effects of biped robots. It is expected that walking speeds of limit cycle walkers would be further improved by adding our proposed mechanism. We are now developing a biped robot with knee joints as shown in Fig. 8 and plan to verify the effectiveness of our proposed method in experiments.

REFERENCES

[1] HONDA, "Humanoid Robot ASIMO," [Online]. Available: <http://www.honda.co.jp/ASIMO/>.
 [2] AIST, "Humanoid robot hrp4-c," [Online]. Available : <http://www.aist.go.jp>.
 [3] PETMAN, "Boston dynamics: Humanoid robot petman," [Online]. Available : <http://www.bostondynamics.com>.
 [4] T. McGeer, "Passive dynamic walking," *The International Journal of Robotics Research*, vol. 9, no. 2, pp. 62–82, 1990.

[5] M. W. Spong, "Passivity based control of the compass gait biped," in *Proc. of IFAC World Congress, Beijing, China*. Citeseer, 1999, pp. 19–24.
 [6] F. Asano, M. Yamakita, and K. Furuta, "Virtual passive dynamic walking and energy-based control laws," in *Proc. IEEE/RSJ International Conference on Intelligent Robots and Systems (IROS)*, 2002, pp. 1149–1154.
 [7] M. Wisse and J. Van Frankenhuyzen, "Design and construction of mike; a 2d autonomous biped based on passive dynamic walking," in *Proc. International Symposium of Adaptive Motion and Animals and Machines (AMAM03)*, 2003.
 [8] M. Wisse, "Three additions to passive dynamic walking; actuation, an upper body, and 3D stability," in *Proc. IEEE/RAS International Conference on Humanoid Robots (ICHR)*, vol. 1, 2004, pp. 113–132.
 [9] D. G. E. Hobbelen and M. Wisse, "Limit cycle walking", *Humanoid Robots, Human-like Machines*, chapter 14. InTech, 2007.
 [10] K. Narioka, S. Tsugawa, and K. Hosoda, "3d limit cycle walking of musculoskeletal humanoid robot with flat feet," in *IEEE/RSJ International Conference on Intelligent Robots and Systems (IROS)*, 2009, pp. 4676–4681.
 [11] S. H. Collins, A. Ruina, R. Tedrake, and M. Wisse, "Efficient bipedal robots based on passive-dynamic walkers," *Science*, vol. 307, no. 5712, pp. 1082–1085, 2005.
 [12] F. Asano and Z. W. Luo, "Efficient dynamic bipedal walking using effects of semicircular feet," *Robotica*, vol. 29, no. 03, pp. 351–365, 2011.
 [13] —, "Energy-efficient and high-speed dynamic biped locomotion based on principle of parametric excitation," *IEEE Transactions on Robotics*, vol. 24, no. 6, pp. 1289–1301, 2008.
 [14] D. Hobbelen and M. Wisse, "Ankle actuation for limit cycle walkers," *The International Journal of Robotics Research*, vol. 27, no. 6, pp. 709–735, 2008.
 [15] —, "Controlling the walking speed in limit cycle walking," *The International Journal of Robotics Research*, vol. 27, no. 9, pp. 989–1005, 2008.
 [16] —, "Swing-leg retraction for limit cycle walkers improves disturbance rejection," *IEEE Transactions on Robotics*, vol. 24, no. 2, pp. 377–389, 2008.
 [17] Y. Hanazawa, H. Suda, and M. Yamakita, "Analysis and experiment of flat-footed passive dynamic walker with ankle inerter," in *Proc. IEEE International Conference on Robotics and Biomimetics (ROBIO)*, 2011, pp. 86–91.
 [18] Y. Hanazawa and M. Yamakita, "High-efficient biped walking based on flat-footed passive dynamic walking with mechanical impedance at ankles," *Journal of Robotics and Mechatronics*, vol. 24, no. 3, pp. 498–506, 2012.
 [19] Y. Hanazawa, H. Suda, Y. Iemura, and M. Yamakita, "Active walking robot mimicking flat-footed passive dynamic walking," in *Proc. IEEE International Conference on Robotics and Biomimetics (ROBIO)*, 2012, pp. 1281–1286.
 [20] L. Rome, L. Flynn, and T. Yoo, "Biomechanics: Rubber bands reduce the cost of carrying loads," *Nature*, vol. 444, no. 7122, pp. 1023–1024, 2006.
 [21] D. Tanaka, F. Asano, and I. Tokuda, "Gait analysis and efficiency improvement of passive dynamic walking of combined rimless wheel with wobbling mass," in *Proc. IEEE/RSJ International Conference on Intelligent Robots and Systems (IROS)*, 2012, pp. 151–156.
 [22] J. W. Grizzle, G. Abba, and F. Plestan, "Asymptotically stable walking for biped robots: Analysis via systems with impulse effects," *IEEE Transactions on Automatic Control*, vol. 46, no. 1, pp. 51–64, 2001.